


RESEARCH ARTICLE | JANUARY 18 2024

Introduction to the new airborne thermal infrared imager VELOX for remote sensing of cloud and surface properties

Michael Schäfer ; Kevin Wolf; André Ehrlich; Evelyn Jäkel; Anna Elisabeth Luebke; Joshua Müller;
Jakob Thoböll; Bjorn Stevens; Manfred Wendisch



AIP Conf. Proc. 2988, 050001 (2024)

<https://doi.org/10.1063/5.0183450>

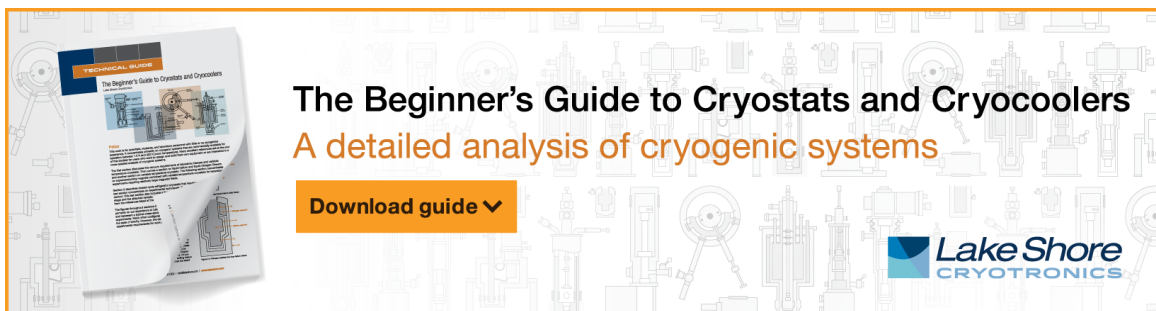


View
Online




Export
Citation

CrossMark



The Beginner's Guide to Cryostats and Cryocoolers
A detailed analysis of cryogenic systems

[Download guide](#)



Introduction to the new Airborne Thermal Infrared Imager VELOX for Remote Sensing of Cloud and Surface Properties

Michael Schäfer,^{1, a)} Kevin Wolf,^{1, 2} André Ehrlich,¹ Evelyn Jäkel,¹ Anna Elisabeth Luebke,¹ Joshua Müller,¹ Jakob Thoböll,¹ Bjorn Stevens,³ and Manfred Wendisch¹

¹⁾Leipzig Institute for Meteorology, Leipzig University, Leipzig, Germany

²⁾Now: Institut Pierre Simon Laplace, Sorbonne Université, Paris, France

³⁾Max Planck Institute for Meteorology, Hamburg, Germany

^{a)}Corresponding author: michael.schaefer@uni-leipzig.de

Abstract. The new airborne thermal infrared imager VELOX (Video airborne Longwave Observations within siX channels) with six spectral bands in the thermal infrared wavelength range from 7.7 μm to 12 μm is introduced. The imager is operated on board the German High Altitude and Long Range Research Aircraft (HALO), measuring two-dimensional (2D) fields of brightness temperature. VELOX was used for the first time during the EUcinating the RoLE of Cloud-Circulation Coupling in ClimAte (EUREC⁴A) campaign. Technical specifications, information on the calibration procedure, and first results from the VELOX broadband channel are presented. VELOX is used to estimate cloud masks/fractions along the flight tracks. For the cloudy parts, 2D fields of the cloud top altitude are derived and analysed. First analysis reveal that the cloud top brightness temperature can be resolved with a thermal resolution of about 0.1 K, which means that the cloud top altitude can be resolved with a vertical resolution of about 40 m.

INTRODUCTION

Multiple studies discuss the advantage of measurements in the thermal infrared (TIR) for remote sensing applications and show that TIR imagery is a powerful technique to study atmospheric and surface properties [1, 2]. Compared to the solar spectral range, three-dimensional (3D) radiative effects like shadowing or multiple-scattering are avoided and the detection of clouds above bright surfaces like snow or sea ice becomes possible [3]. In addition, thermal infrared imagery is sensitive to optically very thin clouds, which are already sub-visible in the solar spectral range and observations are also possible during nighttime [4].

Based on thermal imagery, various retrieval techniques were developed to derive cloud or surface properties [3]. For clouds, these properties include the coverage and thermodynamic phase, particle effective radius and liquid/ice water path, as well as cloud top temperature or height [3, 4, 5, 6]. For the surface properties, products like the surface type and temperature, or the snow grain size can be derived [3, 7]. However, although satellite observations may cover large spatial and temporal scales, they often lack of the required spatial and temporal resolution to investigate small-scale or short-term processes in clouds or of surfaces. Contrarily, airborne observations provide areal measurements with a high spatial resolution down to several meters. Furthermore, satellite sensors often use push-broom sensors, while airborne installations also allow two-dimensional (2D) sensors. Those enable to observe clouds (while passing over) from different viewing directions and to perform 3D reconstructions of the cloud shape. In addition, the revisit frequency over the same target is increased due to the higher mobility of airplanes.

In the following, the six-band and temperature-stabilized TIR imager VELOX (Video airborne Longwave Observations within siX channels) is presented, which was first introduced in [3]. It is based on a commercially available TIR imager, manufactured by the IRCAM GmbH, Erlangen, Germany. The whole system is of small size due to waiving an on-board calibration setup. Instead, the imager is installed in a temperature stabilized housing and post-calibration routines are applied. VELOX is currently operated on the High Altitude and Long range research aircraft (HALO) with the potential to be operated on other platforms as well.

TECHNICAL SPECIFICATIONS AND CHANNEL SELECTION

Major parts of this section were first presented by Schäfer et al. (2022) [3]. The main components of the VELOX system are an actively cooled TIR imager and an un-cooled infrared thermometer, which are installed in a nadir viewing orientation for airborne applications. Thus, they observe the upward spectral TIR radiance emitted by clouds

and surfaces [3]. The TIR imager is operated at 100 Hz temporal resolution and uses 640 by 512 spatial pixels (35.5° by 28.7° field of view). Due to the active cooling of the detector by a Stirling cooler, the Noise Equivalent Differential Temperature (NEDT) is reduced to 40 mK. This improves the performance of the imager and helps to ensure a stable absolute calibration throughout its operation [3].

The imager itself has a broadband detector, measuring between 7.7 μm and 12 μm . Observations at different wavelengths are realized by a synchronously rotating (100 Hz) filter wheel with six slots in front of the detector. For some applications, only the pure broadband measurements are needed, e.g., for sea surface temperature or cloud top altitude retrievals. Therefore, two of the six slots provide broadband measurements (7.7 - 12 μm). The remaining four slots are equipped with spectral filters, specifically selected to match with the current instrumentation of, e.g., MODIS, MSI, and AVHRR and focus on cloud and surface property retrievals. For example, Chylek et al. (2006) [6] revealed very similar slopes of the imaginary part of the refractive index of liquid water and ice in the wavelength range between 8.5 μm and 10 μm , while they are significantly different at wavelengths between 11 μm and 12 μm [3]. Related to this, two channels are selected for VELOX to discriminate between liquid water and ice in clouds. Furthermore, for those two channels the split-window method [5, 8] can be applied to retrieve the cloud effective radius or the liquid water path [4, 9]. With respect to surface property retrievals, e.g., Hori et al. (2006) [7] discussed that the emissivity of snow and ice are very similar at 10.6 μm , while they are significantly different at wavelengths close to 12 μm , where it also depends on the type of snow or ice. This behaviour is used with VELOX to discriminate ocean, snow, and ice surfaces in Arctic regions and to develop a snow-type and snow-grain-size retrieval.

CALIBRATION PROCEDURE

In the following the calibration procedure is outlined. A detailed description of the calibration procedure is discussed in Schäfer et al. (2022) [3]. It provides also information on the validation of the calibration and the sensitivity of the system, which both were analysed using a high-performance black body and cloud free radiative transfer simulations.

Each pixel of the imager provides a digital number, proportional to detected photon counts per unit time [3]. The detected signal depends on the thermal emission of the target, but also on the thermal emission of the environment, including the imager itself. Therefore, several calibration and correction processes are needed to convert the raw counts into radiance I^\uparrow (in units of $\text{W m}^{-2} \text{nm}^{-1} \text{sr}^{-1}$) or brightness temperature T_B (given in units of $^\circ\text{C}$) [3].

The absolute radiometric calibration is performed by the manufacturer, providing calibration coefficients to transform the digital numbers into radiance or brightness temperature. However, these calibration coefficients depend to a certain degree on the environmental conditions during the initial calibration process. Therefore, cross-calibrations are needed to adapt the calibration factors to the environmental conditions during the operation of the imager. This is performed in a post-calibration process after operating the imager in the field by using a high-performance black body in the laboratory of the authors.

Further corrections are non-uniform corrections of the detector and bad-pixel replacements. Both corrections reduce the noise in the images, which is typical for TIR detectors. The non-uniform-correction homogenizes the gain of all pixels among each other to derive an image without artificial noise or stripes. The bad-pixel correction further reduces the noise by replacing poor pixels with an average value derived from the neighboring pixels. Both corrections are performed with a black body, operated at different temperatures.

To the last, the radiative influence of the window that seals the tubular mounting in the case of airborne application needs to be corrected. Several temperature sensors are used to detect the temperature of the window, the mounting, and the imager itself. Using this and the known transmission, emission/absorption and reflection coefficients of the window, its radiation offset to the measurements can be calculated and subtracted.

DATA AND PRODUCTS

Figure 1 exemplary shows a fully calibrated 2D (left) and post-processed push-broom (right) field of brightness temperature of an example measurement, acquired airborne during the EUREC⁴A campaign in 2020. The colder clouds are identified by bluish to greenish colors over the warmer ocean in reddish colors. With the given spatial resolution of about 10 m by 10 m pixel size at 10 km flight altitude the horizontal inhomogeneity of tiny cloud patches smaller than 100 m in diameter is identified. With respect to spatial, temporal, and thermal resolution, such fields of brightness temperature are further discussed in detail in [3].

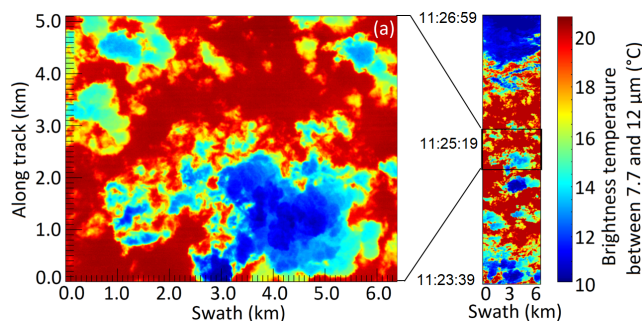


FIGURE 1. The left image shows a fully calibrated two-dimensional field of brightness temperature measured at a flight altitude of approximately 10 km with the VELOX broadband channel during the EUREC⁴A field campaign. The right image illustrates a post-processed push-broom image acquired in a 3 min 20 sec time window around the acquisition time of the left image. Adapted with permission from the publication VELOX – a new thermal infrared imager for airborne remote sensing of cloud and surface properties, by Atmospheric Measurement Techniques, 2022, doi:810.5194/amt-15-1491-2022.

The post-processed push-broom image on the right side in Fig. 1 can be applied to compare or combine the VELOX observation to or with other push-broom sensors like specMACS [10] or nadir pointing active remote sensing instrumentation like the Water vapor Lidar Experiment in Space (WALEs) [11] or the HALO Microwave Package (HAMP) [12]. The comparison between the 2D and push-broom images further allows to identify distortions due to aircraft motions, or to add more observations from different viewing directions to the same scene.

Based on the observed brightness temperature (Fig. 2a), two products are introduced; the cloud mask shown in Fig. 2b and the cloud top altitude shown in Fig. 2c. The cloud mask is derived by the use of a threshold method. The reference for the threshold method originates from an envelope fit to the highest brightness temperature in a specific scene, which represents the cloud-free state. Lower values of the detected brightness temperature compared to this maximum envelope are related to observations of clouds. A detailed description of this method can be found in [3]. Furthermore, using this method, cloud fractions were calculated, which were applied to derive a combined cloud mask with confidence levels of "most likely cloudy", "probably cloudy", "cloud-free", and "unknown", illustrated in Fig. 2b. A comparison to other instruments installed on HALO (specMACS, HAMP, WALEs) reveals a well agreement in the detected cloud fraction throughout the whole campaign [13].

Knowing the pixels, which are identified as cloudy and using comparisons to atmospheric profile measurements from dropsondes and radiative transfer simulations of the cloud free atmosphere, the cloud top altitude is derived. The data reveal the potential of VELOX to resolve the cloud top temperature with a thermal resolution of better than 0.1 K, leading to a cloud top altitude resolution of 40 m. Furthermore, comparisons to the cloud top altitude derived from WALEs results in a well agreement. The detailed description of the cloud top altitude estimation including a sensitivity analysis is given in [3].

CONCLUSION

Based on the publication by [3], the technical specifications, calibration and correction procedures, and products of the new airborne, six-channel thermal infrared TIR imager VELOX (Video airborne Longwave Observations within siX channels) were presented. VELOX measures 2D fields of upward terrestrial radiance or brightness temperature in 640 by 512 spatial pixels (35.5° by 28.7° field of view, 7.7 μm to 12 μm wavelength). It utilizes spectral channels to retrieve cloud and surface properties such as cloud cover, cloud top altitude, phase, liquid/ice water path, effective radius, surface temperature, and snow/ice properties [3].

Two-dimensional images of upward TIR brightness temperature, collected during the EUREC⁴A campaign were presented and discussed together with post-processed push-broom-like images. Both types provide a detailed view on cloud and surface structures with a spatial resolution of 10 m by 10 m at a distance of 10 km. The brightness temperature is used to derive cloud fractions and a combined cloud mask, given in confidence levels of "most likely cloudy", "probably cloudy", "cloud-free", and "unknown". For cloudy parts, the cloud top temperature can be resolved with a thermal resolution of better than 0.1 K. In a basic cloud top altitude retrieval, this translates into a vertical resolution of approximately 40 m [3]. In the near future, it is envisioned to extend the current list of VELOX products by

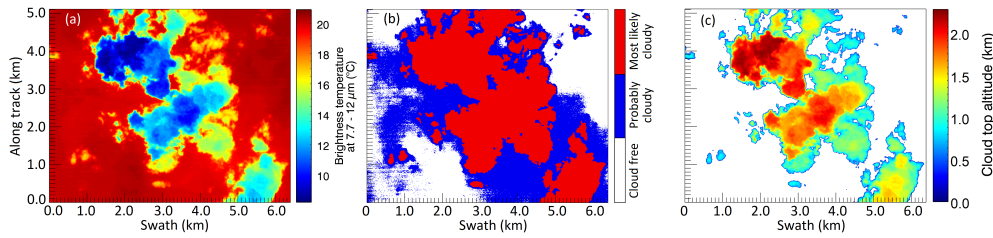


FIGURE 2. (a) Two-dimensional field of brightness temperature measured at a flight altitude of approximately 10 km with the VELOX broadband channel between $7.7\ \mu\text{m}$ and $12\ \mu\text{m}$ during the EUREC⁴A field campaign on 9 February 2020 at 15:05:21 UTC. For the same scene, panel (b) shows the combined cloud mask and panel (c) the retrieved cloud top altitude. Adapted with permission from the publication VELOX – a new thermal infrared imager for airborne remote sensing of cloud and surface properties, by Atmospheric Measurement Techniques, 2022, doi:810.5194/amt-15-1491-2022.

cloud-retrieval products of the cloud phase, effective radius, and liquid/ice water path. Furthermore, surface property retrievals from VELOX shall include products for the sea-surface temperature and snow/ice/water discrimination.

ACKNOWLEDGEMENTS

We gratefully acknowledge the funding by the Deutsche Forschungsgemeinschaft (DFG, German Research Foundation) – Projektnummer 268020496 – TRR 172, within the Transregional Collaborative Research Center “Arctic Amplification: Climate Relevant Atmospheric and SurfaCe Processes, and Feedback Mechanisms (AC)³”. This research was further funded by the DFG (Projektnummer 422897361) within the HALO-SPP 1294.

REFERENCES

1. F. Parol, J. C. Buriez, G. Brogniez, and Y. Fouquart, “Information content of avhrr channels 4 and 5 with respect to the effective radius of cirrus cloud particles,” *J. Appl. Meteorol.* **30**, 973–984 (1991).
2. A. Garnier, J. Pelon, P. Dubuisson, M. Faivre, O. Chomette, N. Pascal, and D. P. Kratz, “Retrieval of cloud properties using calipso imaging infrared radiometer. part i: Effective emissivity and optical depth,” *J. Appl. Meteorol. Clim.* **51**, 1407–1425 (2012).
3. M. Schäfer, K. Wolf, A. Ehrlich, C. Hallbauer, E. Jäkel, F. Jansen, A. E. Luebke, J. Müller, J. Thoböll, T. Rösenthaller, B. Stevens, and M. Wendisch, “VELOX – a new thermal infrared imager for airborne remote sensing of cloud and surface properties,” *Atmos. Meas. Tech.* **15**, 1491–1509 (2022).
4. Y. Someya and R. Imasu, “Cloud screening and property retrieval for hyper-spectral thermal infrared sounders, remote sensing of aerosols, clouds, and precipitation, chapter 8 - cloud screening and property retrieval for hyper-spectral thermal infrared sounders,” Elsevier, 175–187 (2018).
5. G. Brogniez, C. Pietras, M. Legrand, P. Dubuisson, and M. Haefelin, “A high-accuracy multiwavelength radiometer for in situ measurements in the thermal infrared. part ii: Behavior in field experiments,” *J. Atmos. Oceanic Technol.* **20**, 1023–1033 (2003).
6. P. Chylek, S. Robinson, M. K. Dubey, M. D. King, Q. Fu, and W. B. Clodius, “Comparison of near-infrared and thermal infrared cloud phase detections,” *J. Geophys. Res.* **111**, D20203 (2006).
7. M. Hori, T. Aoki, T. Tanikawa, H. Motoyoshi, A. Hachikubo, K. Sugiura, T. J. Yasunari, H. Eide, R. Storvold, Y. Nakajima, and F. Takahashi, “In-situ measured spectral directional emissivity of snow and ice in the $8\text{--}14\ \mu\text{m}$ atmospheric window,” *Rem. Sens. Environ.* **100**, 486–502 (2006).
8. L. M. McMillin, “The split window retrieval algorithm for sea surface temperature derived from satellite measurements,” *Adv. Space Res. Series*, 437–455 (1980).
9. H. Iwabuchi, M. Saito, Y. Tokoro, N. S. Putri, and M. Sekiguchi, “Retrieval of radiative and microphysical properties of clouds from multi-spectral infrared measurements,” *Progress in Earth and Planetary Science* **3**, 2197–4284 (2016).
10. F. Ewald, T. Kölling, A. Baumgartner, T. Zinner, and B. Mayer, “Design and characterization of specmacs, a multipurpose hyperspectral cloud and sky imager,” *Atmos. Meas. Tech.* **8**, 9853–9925 (2015).
11. M. Wirth, A. Fix., P. Mahnke, H. Schwarzer, F. Schrandt, and G. Ehret, “The airborne multi-wavelength water vapor differential absorption lidar WALES: system design and performance,” *Applied. Physics B.* **96.1**, 201–213 (2009).
12. M. Mech, E. Orlandi, S. Crewell, F. Ament, L. Hirsch, M. Hagen, G. Peters, and B. Stevens, “Hamp – the microwave package on the high altitude and long range research aircraft (halo),” *Atmos. Meas. Tech.* **7**, 4539–4553 (2014).
13. H. Konow, F. Ewald, G. George, M. Jacob, M. Klingebiel, T. Kölling, A. E. Luebke, T. Mieslinger, V. Pörtge, J. Radtke, M. Schäfer, H. Schulz, R. Vogel, M. Wirth, S. Bony, S. Crewell, A. Ehrlich, L. Forster, A. Giez, S. G. ans M. Gutleben, M. Hagen, L. Hirsch, F. Jansen, T. Lang, B. Mayer, M. Mech, M. Prange, S. Schnitt, J. Vial, A. Walbröl, M. Wendisch, K. Wolf, T. Zinner, M. Zöger, F. Ament, and B. Stevens, “Eurec4a’s halo,” *Earth Syst. Sci. Data* **13**, 5545–5563 (2021).